International Journal of Composite Materials 2013, 3(6): 181-190
DOI: 10.5923/j.cmaterials.20130306.07

Static, Quasi-Static and High Loading Rate Effects on Graphene Nano-Reinforced Adhesively Bonded Single-Lap Joints

Babak Soltannia, Farid Taheri*

Department of Civil and Resource Engineering, Dalhousie University, Canada

Abstract Crashworthiness, damage tolerance, energy absorption capability and safety are all important factors in the design of light-weight composite structures. Furthermore, in order to make such structures lighter and more resilient, and to avoid stress concentrations that can occur with mechanical fasteners such as bolted or welded joints, it is preferable to mate the structure's various components with adhesively bonded joints. Therefore, a comprehensive understanding of the response of bonded joints subjected to loadings with various rates is of paramount importance in developing reliable structures. In this paper, the effects of high loading rates on the performance of nano-reinforced adhesively bonded single-lap joints with composite adherends are systematically investigated, and will be compared to the static and quasi-static results. Bonded joints mating carbon/epoxy and glass/epoxy adherends were subjected to tensile loadings under 1.5, and 3 mm/min, and very high loading rate of 2.04E+5 mm/min. The high loading rate tests were conducted using a modified instrumented pendulum, equipped with a specially designed impact load transfer apparatus. The results of the high load rate tests revealed the loading rate sensitivity of the adhesive/joints, as well as the positive influence of nano- reinforcement. In all, that overall stiffness and strength of the joints were increased with increasing loading rates and nano reinforcement. It was also recognized that the effect of nano reinforcement in few cases overcame the effect of loading rate, meaning that even small increases in the amount of nano-particles can overcome enormous increases in loading rates using the same epoxy resin base. The observed failure mechanisms were examined with a scanning electron microscope.

Keywords Graphene nanoplatelets, Nano composites, Loading rate, Impact, Single-lap joints

1. Introduction

Adhesively bonded joints (ABJs) are increasingly being used in automotive, marine, offshore, and oil and gas industries to mate both metallic and fiber-reinforced polymer composite (FRP) structural components. Adhesively bonded FRPs offer numerous advantages, including high strength- and stiffness-to-weight ratios, good fatigue and corrosion resistance, controllable damage tolerance, and high energy absorption capability, all of which makes them more efficient compared to other types of mechanical fasteners[1-9]. Crashworthiness, improved damage tolerance, energy absorption capability, and safety requirements are important factors in the design of light-weight composite structures, especially in automotive and marine vessel applications. However, a major concern in the use of adhesives in these applications has been the lack of an adequate database with regards to the performance of ABJ at high rates of loading. Therefore, the mechanical characterization of ABJs at high loading rates is vital for achieving reliable designs.

The cylindrical nano-particles that are most widely discussed in the scientific literature are carbon nanotubes (CNTs), despite the fact that carbon nanofibers (CNFs), which have a larger diameter and are less expensive, are more widely available. Ceramic nanotubes (e.g., zirconia, tungsten disulfide) or whiskers (e.g., silicon nitride, silicon carbide, and alumina) can also be used in these applications.

The use of carbon nanotubes, which are effectively sheets of graphite rolled into tubes[10, 11], was first proposed by Iijima in 1991 and later by Iijima and Ichihashi in 1993. There are two main kinds of carbon nanotubes. One type is single-walled nanotubes (SWNTs), which consist of a single graphene layer typically wrapped into a cylinder with a diameter of 1-2 nm and hemispherical end caps[11, 12]. The other type, known as multi-walled nanotubes (MWNTs), contains a number of coaxial graphene cylinders, each of which has an end cap and an outer diameter of 3-10 nm. Due to weak Van der Waals forces between the layers, the tension loads are carried only by the outer layer of an MWNT, and thus stress will not be transferred to the inner

* Corresponding author:
farid.taheri@dal.ca (Farid Taheri)
Published online at http://journal.sapub.org/cmaterials

layers[13]. The strength of an MWNT has been estimated to be up to 150 GPa and their elastic modulus up to 900 GPa[14], even though they are quite flexible perpendicular to their longitudinal axis[15]. Their superior mechanical characteristics and desirable length-to-diameter ratio make CNTs highly desirable for composite reinforcement. Nevertheless, to completely benefit from the exceptional mechanical properties of CNTs, two important requirements must be met; (i) strong interfacial bonding should exist between the polymer matrix and CNTs[16], and (ii) nano-particles must be dispersed uniformly within the resin.

Hsiao et al. demonstrated that utilizing CNTs in conjunction with an adhesive could improve the mechanical properties of the joint. By adding 5 wt% MWNT to the epoxy adhesive, the shear load was more efficiently transferred to the adherends (cohesive failure), thereby increasing the average shear strength of the bonding by 45.6%. In SWNTs, failure initiated and developed within the adhesive layer[17].

An important factor in the design of lightweight vehicles is the crashworthiness of composite structures. In particular, the structural joints should have the ability to absorb a large amount of energy to accommodate the safety factors and improve passenger safety. To accomplish this, the dynamic behavior of the adhesively bonded joints used in such applications need to be studied, as the effect of loading rate on the response of ABJ would enable us to design structures that would not fail unexpectedly and catastrophically when subjected to high loading rates.

Harris and Adams used a modified Izod pendulum for impact tests to associate the geometry of SLJs with aluminium adherends. Single-lap joints formed by various types of adhesives were tested under quasi-static and impact at a velocity of 1.4 m/s. The results indicated that joint strength was not considerably influenced by high loading rate, and that, for the majority of adhesives, the impact strength was not significantly higher than the static load[18].

The dynamic behavior of ABJs made of graphite/epoxy unidirectional plies was studied by Galliot et al. A drop weight machine was used to subject the specimens to a suddenly-applied tensile load (impact) in order to compare the results to quasi-static test results. The intent was to find the rate-sensitivity of the adhesive. In contrast to the work of Harris and Adams, an average increase of more than 50% in strength was recognized by comparing the impact and quasi-static test results. They showed that the absorbed energy, the failure load, and the stiffness were intensified with increasing loading rate. Nevertheless, the joint behavior remained qualitatively the same under the quasi-static and dynamic loading cases. They noted that the adhesive did not apparently contribute to the energy absorption of the ABJ and that the deformation of the adherend material absorbed the energy. Baseline quasi-static loading tests were also conducted on a universal tensile machine (Instron) at a loading rate of 0.3 mm/min (5×10E-6 m/s).[19]

Goglio and Rosetto used the instrumented pendulum to study the effect of geometrical parameters on the mechanical properties of adhesively-bonded steel joints. In this investigation, they joined the specimen to a swinging hammer while the striker was clamped. The results indicated evolved joint strength under dynamic conditions and showed the significant effect of adhesive thickness[20].

Ger et al. implemented a “slingshot type” high velocity loading machine to validate the dynamic tensile behavior of composite laminates. The results indicated that the dynamic loading rate could lead to drastic failure. They also mentioned that the dynamic failure load was higher than the quasi-static one[21].

By using a drop weight tower to develop a high loading rate and by conducting quasi-static tests, Brown et al. showed that the compressive and tensile strengths and the modulus were enhanced by increasing loading rates. The tests were performed on an Instron™ electro-mechanical universal test machine at a crosshead speed of 5 mm.min−1 [22].

Hsiao et al. experimentally investigated the effect of CNTs on the performance of ABJs consisting of carbon fiber-reinforced composites. They reported that, by adding only 1 wt% of MWNT in epoxy adhesive, the shear strength of the joint was increased by 31.2%; furthermore, by adding 5 wt% MWNT, the shear strength was increased by 45.6%[17].

It is important to note that there is an optimum amount of nanofiller for which adhesive properties can be maximized. At a higher content, the properties degrade due to changes in the failure mode of the joints. Such degradation could occur in conventional compositesdue to the resulting reduction in the loadbearing area in the resin as a result of excessive amount of added particles occupying the area. In this case, however, it is believed that the resulting degradation could be due to the fact that nano-particles’ dispersion becomes affected at higher content by clustering of the nano-particles. This occurs mainly during the mixing, when electromagnetic forces cause clustering of the particles when they are used above a critical amount. Commonly, the bonded joints with neat adhesives fail at the interface, while nano-reinforced adhesively bonded joints exhibit a cohesive failure mode that occurs within the adhesive. However, at relatively high quantities of nano-reinforcement, the joint failure mode becomes interfacial again. It is clear that MWNT particles enhance the strength and toughness of epoxies because nano-particles strengthen the polymeric chains of the resin and resist crack initiation and propagation[23].

In 2011, Srivastava investigated the effect of adding 3% MWNT to ABJs using a variety of substances as adherends. The results generally showed that the toughness and strength of the epoxy resin had increased; however, it was also demonstrated that the interface bonding strength of ABJs with similar adherends was much higher than those with dissimilar adherends[24].

As the overall goal of our study is to develop a relatively

inexpensive and strong adhesive for common engineering applications where relatively thicker bond-lines are required (unlike the aerospace related applications), various aspects of such ABJ will be investigated. In this work, the effect of high loading rate on the mechanical response of nano-reinforced adhesively bonded single-lap joints with composite adherends subjected to a high load rate at 2.04E+5 mm/min is investigated and results will be compared with those one obtained from static and quasi static tests under 1.5 and 3.0 mm/min. Unidirectional graphite epoxy and E-glass fiber reinforced epoxy laminate were used to fabricate the adherends. The high loading rate tests were accomplished using a modified instrumented pendulum equipped with a specially designed tension impact apparatus. The static and quasi static tests were conducted on a servo universal tensile machine (Instron).

The observed failure mechanisms obtained from the scan electron microscopic study of the failed specimens will also be presented.

2. Experimental Investigation

2.1. Fixture Design

The tensile impact fixture's elements are illustrated in Figure 1, and the actual fixture is shown in Figure 2.

As can be seen, the rod which has been designed to transfer the tensile impact load is aligned within several ball-bearings. To reduce the errors related to undesirable friction during the test, the height of each bolt was adjusted. Furthermore, to avoid unwanted torsions or bending moments, the system was designed with just one degree of freedom and axial movement capability only.

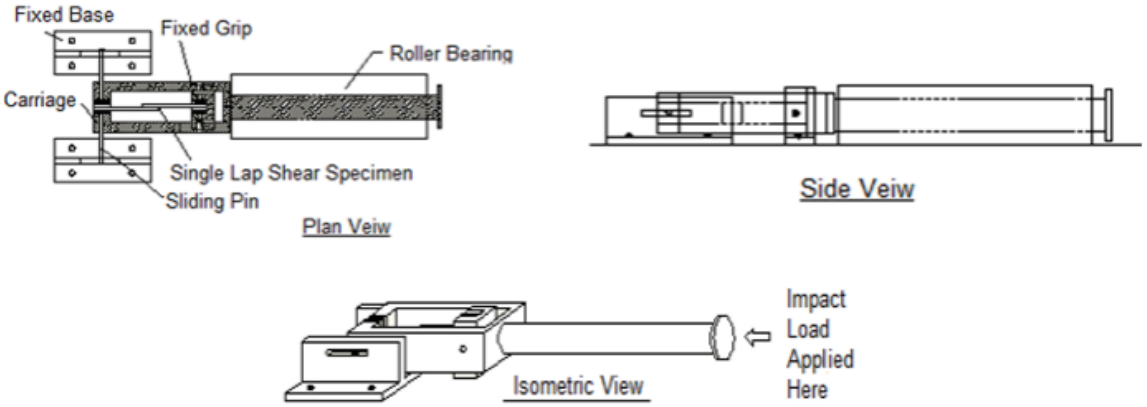

Figure 1. Various views of the fixture used to apply a high speed load to the ABJ

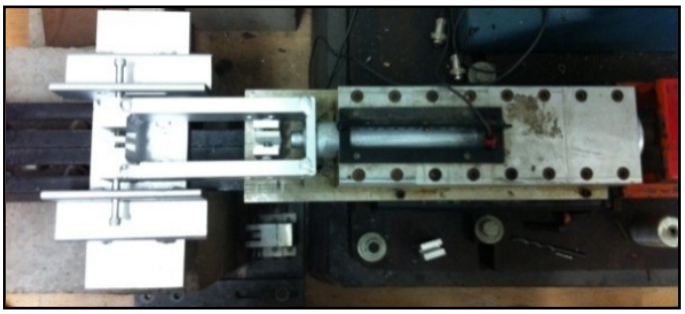

Figure 2. Plan view of the high speed load transfer fixture

A jig was also designed and fabricated to make ABJs consistent and accurately aligned, as shown in Figure 3. Shims were used to obtain the required thickness of the bond-line (i.e., 0.25 mm). This thickness was selected based on ASTM D5868-01standards[35].

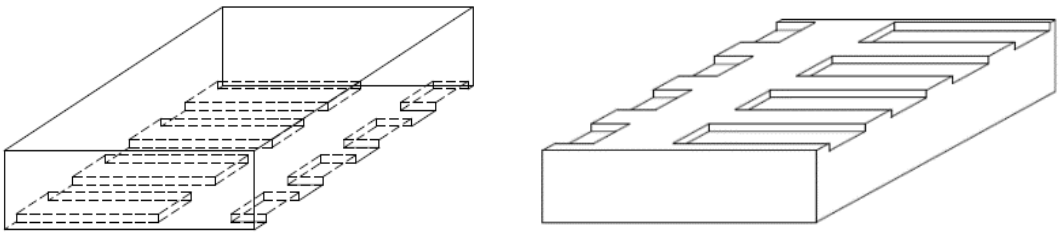

Figure 3. Two halves of the jig made to facilitate fabrication of consistent single-lap joints

2.2. Specimen Preparation

2.2.1. Q-Cell Reinforced Adhesive

To prepare single-lap joints (SLJs), a commonly used thermoset epoxy resin (i.e., West System's 105 resin and 206 hardener[Bay City, MI]) was used as the baseline adhesive, due mainly to its common use and relatively low cost. However, as the viscosity of 105 resin is very low, it must be thickened (i.e., become paste-like) in order to be able to form practical bonded joints. To accomplish this, Q-Cell filler (obtained from Rayplex, Toronto, ON) was used to thicken the resin. Q-Cell is relatively inexpensive and lightweight filler that consists of white hollow inorganic microspheres with low bulk density. It is commonly added to resins at ratios of 0.5% - 10% (by weight). Although it is commonly known that the inclusion of filler will degrade a resin's mechanical properties, nevertheless no factual information or data on the actual level of resin degradation resulting from the addition of Q-Cell filler could be obtained from either the vendor or the literature.

Therefore, in order to establish the level of degradation in the resin properties that the addition of Q-Cell filler would cause, influence of three concentrations of the filler (i.e., 0%, 5%, and 10% by weight Q-Cell) in the resin were investigated. These ratios were selected based on the ease of applying the resin/adhesive in practical applications, especially when adhesives have to be applied on vertical surfaces.

To get a better feeling for and understanding of the strength of the nano-reinforced SLJs, a thermoplastic adhesive (two-part acrylic epoxy) (i.e., Plastic Welder [Devcon, Danvers, MA]) was applied.

2.2.2. Nano Particle-reinforced Adhesive

Since the addition of commonly used fillers like Q-cell is known to degrade the mechanical properties of resins and adhesives, another filler-type material was used with the aim of actually enhancing the resin's mechanical properties. For that, and as a means to economically enhance the mechanical properties of the thermoset resin/adhesive (in our case, West System 105), attempts were made to use various forms of nano-carbons as the filler. However, the uniform dispersion of nano-carbon in resin is quite challenging, time-consuming and thus an added cost. Not only does the dispersion directly govern the mechanical properties of the adhesive, but more importantly, the nano-particles agglomeration causes severe statistical inconsistencies in the strength and performance of adhesives. Therefore, a mechanical stirrer and three-roll mill machine were used to disperse the nano-particles uniformly in the resin.

To enhance dispersion, each roller should revolve with a set constant speed. In this study, the roller speed and calenderingfrequency were set to the maximum speed of the machine (i.e., 174 RPM). To maximize the quality of dispersion, calenderingwas conducted seven times. After each round of calendering, the quality of the dispersion was monitored by sampling the mix and assessing the uniformity of the dispersion with a digital microscope, thereby avoiding unwanted agglomerations.

Three different types of nano-particles were selected to be dispersed into the epoxy resin.

(i) Graphene Nano Platelet (GNP-M-25) with an average diameter of 25 μm, a thickness of 6 nm, and a surface area of 100 m^2/g (obtained from XG Science Ltd., Lansing, MI).

(ii) Multi-Walled Carbon Nanotubes (MWCNTs) with an outer diameter of 5 to 15 nm and more than 95% purity (obtained from the US Research Nanomaterials, Inc., Houston, TX).

(iii) Graphitized Carbon Nano Fibers (CNF) with an outer diameter of 200 to 600 nm and more than 99.9% purity (obtained from the US Research Nanomaterials, Inc., Houston, TX).

The nano-particles were first distributed in the resin using a mechanical stirrer set at a speed of 2000 rpm for 10 min.

The next step was to calender the nano-particle resin slurry using the three-roll mill. The roller gap was set at 20 μm using a filler gauge, for a 0.5% (by weight) concentration of CNF, MWCNT, and GNP (see Figure 4). Later, due to required comparisons, other weight percentages of GNP were taken into consideration (i.e., 0.5%).

Figure 4. The three-roll mill equipment used in the calenderingprocess

As stated, after each calendering, the quality of the dispersion was monitored by taking a small sample and examining the nano-particle dispersion using a digital microscope (see Figure 5).

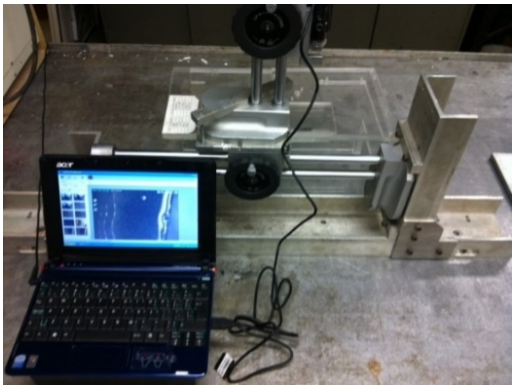

Figure 5. Quality control using a microscope after each calendering

Figure 6 shows small samples of adhesive after addition of nano-particles, captured by digital microscope after each calendering trial. The figures illustrate the advancement of nano-particle dispersion. As it can be seen, Figure 6 (a), which shows the result of the first calendering cycle, reveals tremendous amount of agglomeration. No significant change can be seen upon the completion of the second cycle. However, after each subsequent cycles the visible agglomerations starts to disappearing.

After the above procedures, the curing agent or hardener was added to the slurry and mixed in using the stirrer at a speed of 400 rpm for 4 to 6 minutes. The mixture was then degassed under 28" Hg vacuum for 2 to 3 minutes (the degassing duration depends on the gel time of the resin). After degassing, the mixture was poured in appropriately shaped molds and allowed to cure for 12 hours at room temperature. Typical final products in the form of dog-bone coupons, with dimensions as per ASTM D638-94B, are shown in Figure 7[36].

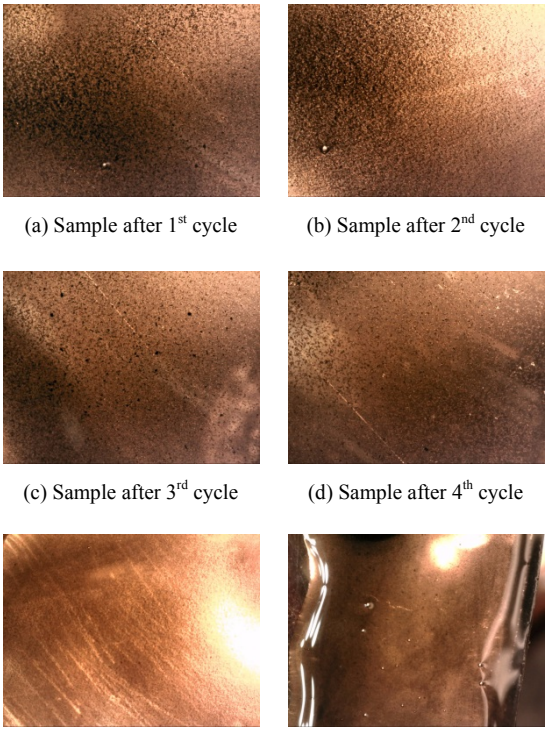

(a) Sample after 1st cycle (b) Sample after 2nd cycle

(c) Sample after 3rd cycle (d) Sample after 4th cycle

(e) Sample after 5th cycle (f) Sample after 6th cycle

Figure 6. Advancement of nano-particles dispersion after each calendering cycle

2.2.3. Adherends Preparation

To manufacture the adherends, laminate plates with a dimension of 350 mm × 350 mm were fabricated by the vacuum resin infusion technique (VRIT). Appropriately-sized coupons were then extracted from the plates, followed by the surface preparation process applied to the bonding regions[29-31]. To meet ASTM D5868-01 requirements, the graphite/epoxy and glass/epoxy plates were made from 12 unidirectional plies. Unidirectional graphite and E-glass fabrics and Huntsman's Araldite LY 564 epoxy resin with Aradure 2954 hardener (West Point, GA) were used to fabricate the laminate plates[35].

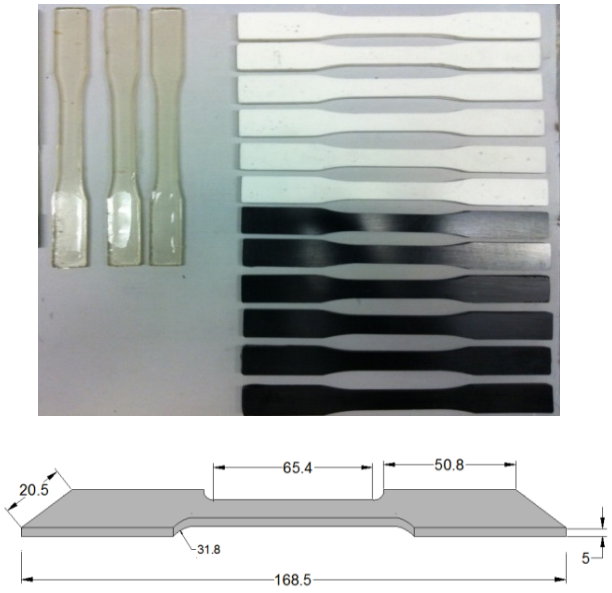

(Dimensions in mm)

Figure 7. Representatives tensile coupons neat, Q-Cell filler and nano-particle reinforced resins, as per ASTM D 638-94B

2.2.4. Single-lap Joint Preparation

Using the described jig, single-lap joints (SLJs) were prepared from graphite/epoxy, glass/epoxy laminate adherends, and adhesive containing different amounts of micro- and nano-particles. Some typical graphite/epoxy and glass/epoxy SLJ specimens are illustrated in Figure 8.

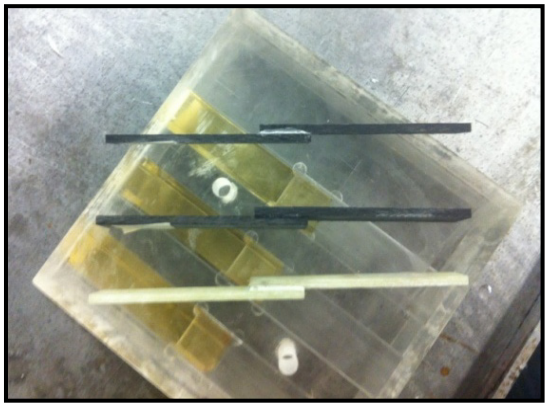

Figure 8. Typical graphite/epoxy and glass/epoxy SLJ specimens

To ensure the adhesive in ABJs would be subjected to concentric load, FRP tabs with appropriate thickness were affixed to adherends' ends (see Figure 9).

It should be noted here that for the high loading rate tests, modified quasi-isotropic tabs with holes in their centres were used (see Figure 10) to prevent slippage and tearing-off of the adherends (see Figure 11). Details of the static, quasi-static and high rate loading for the SLJ specimens are given in next section.

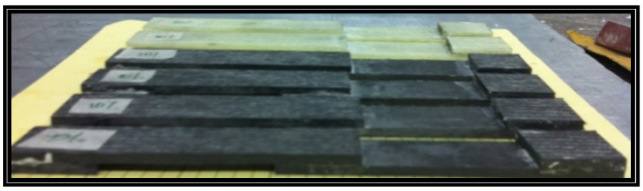

Figure 9. Typical single-lap joint specimens (dimensions in mm)

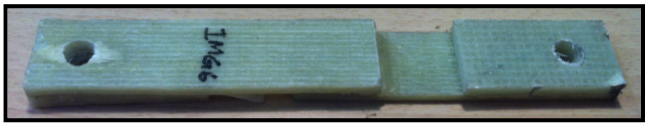

Figure 10. Modified quasi-isotropic tab with holes, designed for high rateloadings

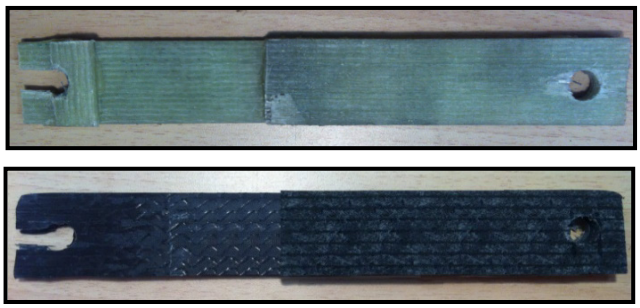

Figure 11. Tearing-off problems in SLJs that were without quasi-isotropic tabs as a result of being subjected to the highrate loading

2.3 Characterization of the Mechanical Properties of Adhesives

The prepared dog-bone shaped specimens were tested in tension using an Instron servo-hydraulic universal test machine equipped with 8500+ electronics. The specimens were subjected to displacement controlled tensile loading, as per ASTM D638, to establish the stress-strain curve of each adhesive[36]. An Instron extensometer was used to record the gauge-length displacement (hence, the strain) of the specimens. First Tensile tests were performed on the neat resin, at room temperature at cross-head speeds of 1.5, 3, 15, and 150 mm/min (as the baseline tests for the static and quasi-static loading conditions), and at 1500 mm/min (as baseline tests for the high loading rate loading condition), based on ASTM D 897 and ASTM D 950, respectively [39-41]. Subsequently, the reinforced-adhesive specimens underwent similar tests. Using the recorded load and gauge length displacement, the stress-strain curve of each adhesive was constructed and their elastic modulus was evaluated.

3. Experimental Investigation of ABJs

The experimental part consists of two phases, as discussed below.

3.1. Baseline Tests

To perform the baseline tests on the ABJs and the dog-bone shaped tensile coupons, the aforementioned loading rates were used. The applied load was recorded directly through the Instron machine's electronics and indirectly using the National Instrument DAQ system equipped with Lab View software. Gauge length displacement was also captured using a laser extensometer through the same DAQ system.

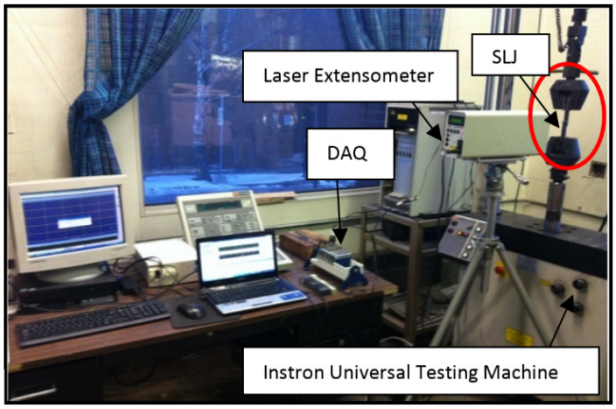

Figure 12. Experimental set-up of static and quasi-static tests

3.2. High Loading Rate Tests

In this category of tests, the applied load was measured using a PCB dynamic load cell (Depew, NY), positioned at the tip of the tensile carriage fixture (see Figure 13(b)). The relative displacement of the overlap region was captured by a dynamic linear variable differential transducer - DLVDT (Data Instruments, Acton, MA), as shown in Figure 13(c). The velocity of the impactor was also measured and adjusted using flat proximity sensors (Omron Corporation, Japan), as shown in Figure 13(a).

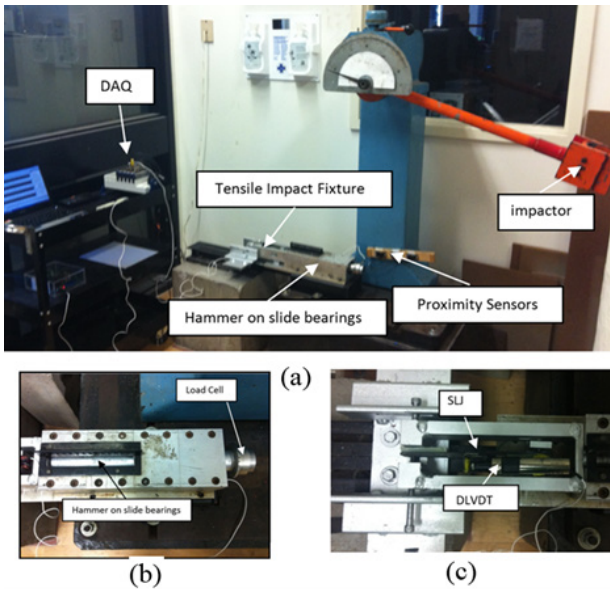

Figure 13. The experimental test set-up for the high loading rate

4. Results and Discussion

The obtained experimental results related to the mechanical properties of adhesives (base-line tests) are shown in Table 1. As indicated, the results can be discussed from two significant points of view.

4.1. Influence of the Micro-filler and Nano-particles on the Mechanical Response of the Adhesives

In light of the main objective of this research, and in an attempt to produce a strong and viscous adhesive from a commonly used and relatively inexpensive room-cured resin, Q-Cell filler and various nano-carbons were added to the neat resin (West System 105). The results of the tensile tests showed that although adding Q-Cell filler increased the adhesive's workability (viscosity), however, the mechanical properties of the adhesive were degraded. The observed decrease in Q-Cell-added adhesive renders the adhesive unsuitable for practical bonding.

Table 1. Effect of nano reinforcement on the average ultimate tensile stress (MPa) in the West System (WS) epoxy adhesive

Loading Rate (mm/min)	Neat WS	WS with 0.25% wt GNP	WS with 0.5% wt GNP	WS with 1.0% wt GNP
1.5	51.12	54.62	55.84	57.15
15	60.87	66.28	67.24	68.36
150	69.33	76.69	78.16	80.17
1500	75.88	84.68	87.24	90.35

In contrast to the above, very good results were obtained when the least expensive type nano-carbon (i.e., graphene nano-platelets - GNP) was added to the resin[33, 34],[43, 44]. Various researchers have also observed that the addition of Carbon Nano Fibers (CNF) or Multi-Walled Carbon Nano Tubes (MWCNTs) to resins have produced enhancement of the resin's mechanical properties and fracture toughness [17-24]. However, very limited data exists for the level of enhancement that could be expected by the addition of GNPs to resins. As stated, GNPs are considerably less expensive than CNFs and MWCNTs. The results indicate that not only does the inclusion of GNPs improve the mechanical properties of this adhesive, it also enhances the resin's viscosity by thickening the resin and making it more workable (less runny) for bonding. This makes it suitable for use as an adhesive, especially for marine and other light-weight applications. In fact, the average ultimate tensile strength of the reinforced adhesive with 0.5% GNPs in weight was enhanced by 9% for lower and 15% for higher rates. Also, as shown in Table 1, he average ultimate tensile strength of reinforced adhesive with 1% GNPs in weight was improved by 12% and 19% for the lower and higher loading rates, respectively (see Figure 14).

Elastomeric particles (fillers or additives) would stretch as they bridge through a propagating crack, resulting in dissipating a portion of the energy required to develop the new surfaces of the growing crack. This, in turn, leads to increasedstrength under higher rate of loading. Figures 15 (a) and (b) illustrate SEM images of the GNP powder and MWCNT. The sizes of the nano-particles can easily be estimated from these figures. For instance, it can beseen that GNPs have an average diameter of approximately 25 μm. This relatively large surface aspect ratio offers added strength to the matrix to resist micro-cracking, and in turn suppresses the advancement of the microcracks.

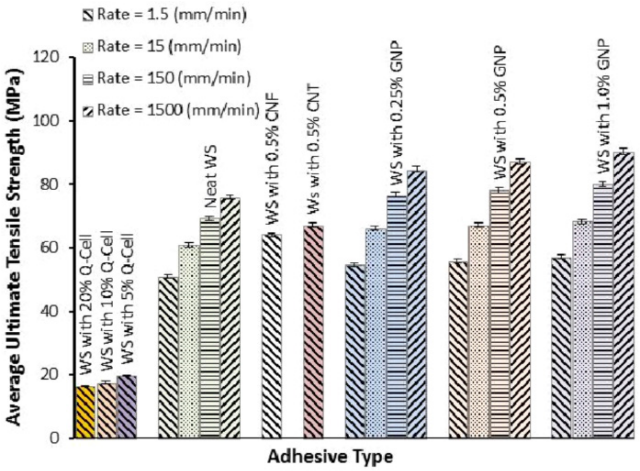

Figure 14. Effects of the Q-Cell and various types of nano-carbon particles on resin's ultimate tensile strength

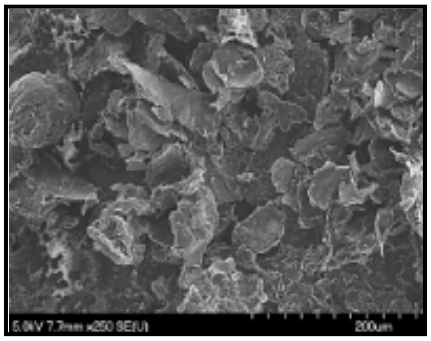

(a)

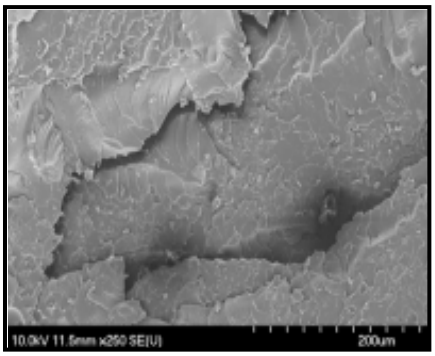

(b)

Figure 15. SEM images of two different nano-particles used for reinforcing the resin

Figure 16 shows typical images of GNPs within the resin. Distinct microcracks, identified by the white arrows, can be seen in this figure. It can also be seen from the figure that GNPs are relatively uniformly dispersed within the resin, as opposed to be piled on top of one another.

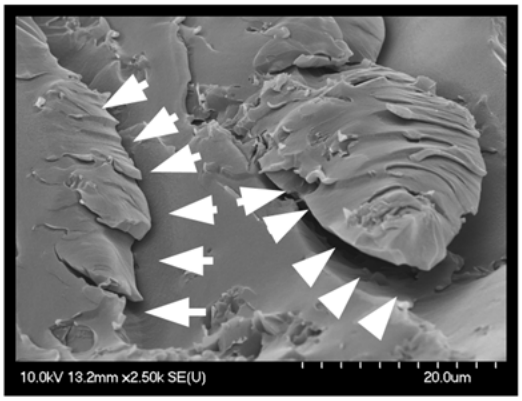

Figure 16. SEM image of resin reinforced GNP hosting microcracks

4.2. Influence of Loading Rate on the Mechanical Response of Nano-particle-reinforced SLJs

As discussed in the previous section (3.2.4), the prepared SLJ specimens were tested using a modified instrumented pendulum equipped with a specially designed high load rate transfer apparatus, subjected to a loading rate of $2.04 \cdot 10^5$ mm/min.

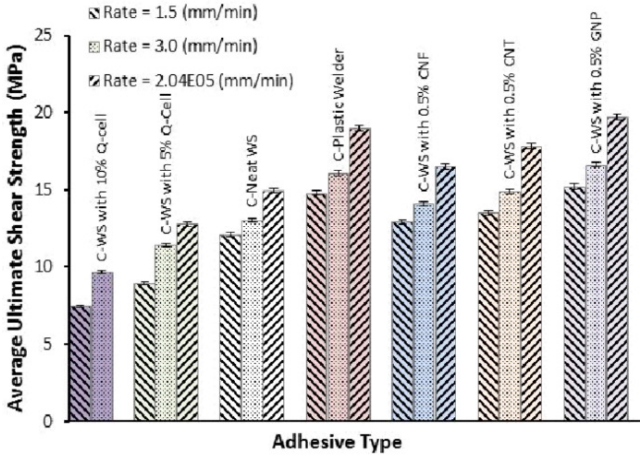

Figure 17. Effects of loading rate on nano-reinforced adhesively bonded single-lap joints with graphite/epoxy adherends

The results showed that the inclusion of GNP in the resin could significantly improve the resin's stiffness and strength. The average ultimate shear strength of SLJs with carbon adherends was increased (relative to the neat adhesive) as much as 32% when SLJs were subjected to the high loading rates and about 26% under quasi-static rates (see Figure 17). It was observed that increases in the loading rates affect the average ultimate shear stress of the adhesive in a nonlinear manner. These enhancements changed in the case of SLJs with glass/epoxy adherends. In that case, the average ultimate shear strength was increased by 28% and 22% for higher and lower loading rates, respectively (see Figure 18). To gain a better understanding of the strength of nano-reinforced adhesives, a thermoplastic adhesive (two-part acrylic epoxy) was also used to prepare SLJ specimens. These specimens also contained the same fillers with the same weight percentages as used in the case of the thermoset resin.

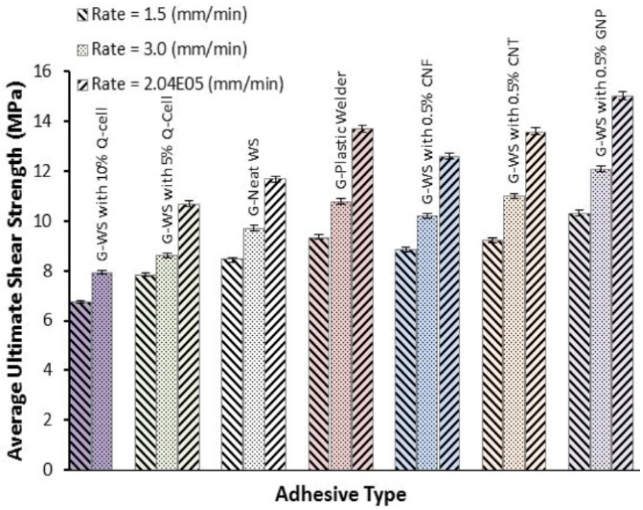

Figure 18. Effects of loading rate on nano-reinforced adhesively bonded single-lap joints with glass/epoxy adherends

It should be mentioned here that, from a macro-molecular point of view, loading rates affect failure modes as well. Figure 19 illustrates the differences between failure modes in static (quasi-static) and higher loading rates. As is shown, the detached cohesive parts that remained on the adherends in the bonded zone were divided into almost two equal portions and the failure occurred at the middle at static and quasi-static load rates; whereas in the case of higher loading rates, the failure occurred at the end of the bond-line, and so the detached portions are not the same.

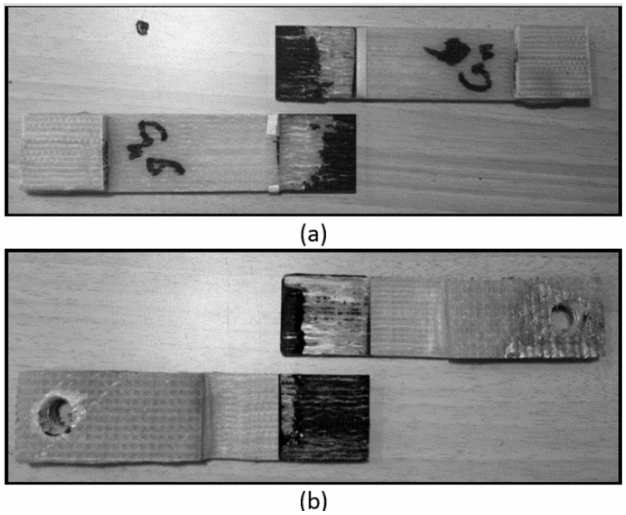

Figure 19. Effects of loading rate on failure modes in SLJs (a) typical failure mode observed under static and quasi-static loading rates (b) at the higher loading rate

Furthermore, as it is shown in Table 2, the average ultimate shear stress of SLJs with carbon adherends are generally higher than the one with glass adherends, which can be explained based on higher strength and stiffness of carbon adherends to flexural and bending moments.

Table 2. Effect of adherend type on the average ultimate shear stress (MPa) of SLJs under different loading rates

Adherend Type	Static test with rate of (1.5 mm/min)				
	WS* with 5% Q-Cell	Neat WS	WS with 0.5% CNT	WS with 0.5% GNP	PW**
Graphite-Epoxy	8.95	12.10	13.51	15.20	14.98
Glass-Epoxy	7.84	8.44	9.25	10.32	9.35
High loading rate (2.04E05 mm/min)					
Graphite-Epoxy	14.93	14.93	17.82	19.70	18.23
Glass-Epoxy	10.70	11.70	13.60	15.03	13.70

*WS stands for the West System
**PW stands for the Plastic Welder

5. Conclusions

The results indicated that ABJs tested under the highest loading rates exhibited increased stiffness and strength. It was also observed that 0.25% GNP (in weight) has approximately the same mechanical properties of 0.5% CNF and CNT (in weight) under the same loading rate. It was also shown that 0.5% GNP (in weight) under lower loading rates exhibited similar mechanical behavior as 0.25% GNP (in weight) subjected to the highest loading rate. It was also concluded that ABJs with carbon adherends show higher strength in comparison with the one with glass adherends. Also, it was concluded that by increasing the loading rate, the average ultimate shear and tensile strength and stiffness generally were enhanced. Loading-rate-dependent properties derived from the experimental data will be used in the near future in conjunction with finite element analysis to conduct a parametric study and optimize the performance of such joints.

The other experimental observations of this investigation are as follows:

The results of the tensile tests on neat adhesive coupons showed that although adding Q-Cell filler increased the adhesive's workability (viscosity), however, it led to gradation of adhesive's mechanical properties. The observed response as a result of addition of the Q-Cell renders the adhesive unsuitable for practical bonding.

In contrast to the above, very good results were obtained when the relatively inexpensive type of nano-carbon (i.e., graphene nano-platelets - GNP) was added to the resin. It was also observed that the addition of Carbon Nano Fibers (CNF) or Multi-Walled Carbon Nano Tubes (MWCNTs) to resins improved the resin's mechanical properties, but not to the same degree as the GNP did.

It was also demonstrated that the increase in loading rate resulted to higher apparent strength of ABJs. This increase was even more significant than the enhancement obtained by inclusion of the nano-carbon particles.

ABJs with graphite/epoxy adherends showed higher strength and stiffness compared to the ones with glass/epoxy adherends. This increase is attributed to the fact that graphite/epoxy adherends are comparativelysignificantly stiffer than glass/epoxy adherends, and consequently, the bending moments at the overlap region (hence the shear and peel stresses) are minimized.

ACKNOWLEDGEMENTS

The financial support of the NSERC in support of this work is gratefully acknowledged.

REFERENCES

[1] L.F.M. da Silva, A. Ochsner and R.D. Adams, Handbook of adhesion technology. Springer-Verlag, Berlin, Heidelberg (2011).

[2] E.M. Petrie, Handbook of adhesives and sealants. McGraw-Hill, New York (2000).

[3] A.J. Kinloch, Adhesion and adhesives: science and technology. Chapman & Hall, London (1987).

[4] R.D. Adams, J. Comyn and W.C. Wake, Structural adhesive joints in engineering, 2nd edition. Chapman & Hall, London (1997).

[5] J-M. Berthelot, Composite materials, Mechanical behavior and structural analysis. New York: Springer (1999).

[6] M.W. Hyer, Stress Analysis of Fiber-Reinforced Composite Materials. McGraw-Hill Inc., New York (1998).

[7] J. N. Reddy, Theory and Analysis of Elastic Plates and Shells CRC, 2nd edition. Taylor & Francis, Philadelphia, PA (2006).

[8] S. Timoshenko and S. Woinowsky-Krieger, Theory of Plates and Shells 2nd Ed., McGraw-Hill, New York (1959).

[9] M.D. Banea and L.F.M. da Silva, Adhesively bonded joints in composite materials: an overview, Journal of Materials: Design and Applications, vol. 233, pp. 1-18 (2008).

[10] S. Iijima, Helical microtubules of graphitic carbon. Journal of Nature, vol. 354, pp.56-58 (1991).

[11] S. Iijima and T. Ichihashi, Single-shell carbon nanotubes of 1-nm diameter. Journal of Nature, vol. 363, pp. 603-605 (1993).

[12] S.C. Tjong, Structural and mechanical properties of polymer nanocomposites. Journal of Material Science and Engineering, vol. 53, Issue (3-4), pp. 73-197 (2006).

[13] K.T. Lau, C. Gu, G.H. Gao, H.Y. Ling and S.R Reid, Stretching process of single- and multi-walled carbon nanotubes for nanocomposite applications. Journal of Carbon, vol. 42, Issue (2), pp. 426-429 (2004).

[14] B.G. Demczyk, Y.M. Wang, J. Cumings,M. Hetman,W. Han, A. Zettl and R.O. Ritchie, Direct mechanical measurement of the tensile strength and elastic modulus of multiwalled carbon

nanotubes. Journal of Material Science and Engineering, vol. 12, pp. 934-935 (2002).

[15] R. Saito,G. Dresselhaus and M.S. Dresselhaus Physical properties of carbon nanotubes. Imperial College Press, London (1998).

[16] M. Alexandre and P. Dubois, Polymer-layered silicate nanocomposites: preparation, properties and uses of a new class of materials. Journal of Material Science Engineering Reports, vol. 28, Issue (1-2), pp.1-63 (2000).

[17] K.T. Hsiao, J. Alms and S.G. Advani Use of epoxy/ multiwalled carbon nanotubes as adhesives to join graphite fiber reinforced polymer composites. Nanotechnology, vol. 14, Issue (7), pp. 791-793 (2003).

[18] J.A. Harris and R. Adams, An assessment of the impact performance of bonded joints for use in high energy absorbing structures. Proc International Mechanical Engineering, vol. 199(C2), pp. 121-131 (1985).

[19] C. Galliot,J. Rousseau and G. Verchey, Drop weight tensile impact testing of adhesively bonded carbon/epoxy laminate joints. International Journal of Adhesion and Adhesives, vol. 35, pp. 68-75 (2012).

[20] L. Goglio and M. Rossetto Impact rupture of structural adhesive joints under different stress combinations. International Journal of Impact Engineering, vol. 35, Issue (7), pp. 635-643 (2008).

[21] G.S. Ger, K. Kawata and M. Itabashi, Dynamic tensile strength of composite laminate joints fastened mechanically. Journal of Theoretical and Applied Fracture Mechanics, vol. 24, Issue (2), pp. 147–155 (1996).

[22] Kevin, K.A.Brown, R.Brooks and N.A. Warrior,The static and high strain rate behavior of a commingled E-glass/ polypropylene woven fabric composite. Composites Science and Technology, vol. 70, Issue (2), pp. 272-283 (2010).

[23] V.K. Srivastava and P.J. Hogg, Moisture Effects on the toughness, mode-I and mode-II of particles filled quasi-isotropic glass-fibre-reinforced polyester resin composites. Journal of Material Science. vol. 33, Issue (5), pp. 1129–1136 (1998).

[24] V.K. Srivastava, Effect of carbon nanotubes on the strength of adhesive lap joints of C/C and C/C–SiC ceramic fibre composites. International Journal of Adhesion and Adhesives, vol. 31, Issue (6), pp. 486–489 (2011).

[25] G.C. Jacob, J.M. Starbuck, J.F. Fellers and S. Simunovic, Strain rate effects on the mechanical properties of polymer composite materials. Journal of Applied Polymer Science, Vol. 94, pp. 296-301 (2004).

[26] R.L. Sierakowski, Strain rate effects in composites. Journal of Applied Mechanics Review, vol. 50, pp. 741-761 (1999).

[27] S. Barre,T. Chotard and M.L. Benzeggagh, Comparative study of strain rate effects on mechanical properties of glass fiber-reinforced thermoset matrix composites. Journal of Composite: Applied Science Manufacturing, vol. 27, pp. 1169-1181 (1996).

[28] M.S. Hamouda and M.S.J. Hashmi, Testing of composite materials at high rates of strain: advances and challenges. Journal of Material Processing Technology, vol. 7, pp. 327-336 (1998).

[29] M.J. Davis and D. Bond, Principles and practice of adhesive bonded structural joints and repairs. International Journal of Adhesion and Adhesives, 19(3), 91-105 (1999).

[30] P. Molitor, V. Barron and T. Young, Surface treatment of titanium for adhesive bonding to polymer composites: a review. International Journal of Adhesion Adhesives, vol. 21, Issue (2), pp. 129-136 (2001).

[31] J.S. Kim and D.H. Reneker, Mechanical properties of composites using ultrafine electrospun fibers. Journal of Polymer Composites, vol. 20, Issue (1), pp. 124-131 (1999).

[32] J.A. Chambers, Preloaded Joint Analysis Methodology for Space Flight Systems. NASA TM-106943 (1995).

[33] R.N. Rothon and M. Hancock, General principles guiding selection and use of particulate materials. In: Particulate-filled polymer composites. Rothon R. N. (ed) Longman Scientific and Technical, Harlow, P1 (1995).

[34] R. Senguptaa, M. Bhattacharyaa, S. Bandyopadhyayb and A.K. Bhowmicka, A review on the mechanical and electrical properties of graphite and modified graphite reinforced polymer composites, Journal Polymer Science, vol. 36, pp. 638-670 (2011).

[35] Standard Test Method for Lap Shear Adhesion for Fiber Reinforced Plastic (FRP) Bonding, ASTM International, West Conshohocken, ASTM D5868-01 (2012).

[36] Standard Test Method for Tensile Properties of Plastics, ASTM International, West Conshohocken, ASTM D638 (2012).

[37] Terminology of Adhesives, ASTM International, West Conshohocken, ASTM D907 (2012).

[38] Guide for Use of Adhesive-Bonded Single-lap-Joint Specimen Test Results, ASTM International, West Conshohocken, ASTM D4896 (2012).

[39] Test Method for Tensile Properties of Adhesive Bonds, ASTM International, West Conshohocken, ASTM D897 (2012).

[40] Test Method for Strength Properties of Adhesive Bonds in Shear by Compression Loading, ASTM International, West Conshohocken, ASTM D905 (2012).

[41] Test Method for Impact Strength of Adhesive Bonds, ASTM International, West Conshohocken, ASTM D950 (2012).

[42] Test Method for Apparent Shear Strength of Single-Lap-Joint Adhesively Bonded Metal Specimens by Tension Loading (Metal-to-Metal), ASTM International, West Conshohocken, ASTM D1002 (2012).

[43] Kaneka, http://www.kaneka.com.Retrieved (2012).

[44] Sigma Aldrich, http//www.sigmaaldrich.com (2012).